



## Atomic layer deposited Al<sub>2</sub>O<sub>3</sub> passivation of type II InAs/GaSb superlattice photodetectors

Omer Salihoglu, Abdullah Muti, Kutlu Kutluer, Tunay Tansel, Rasit Turan et al.

Citation: *J. Appl. Phys.* **111**, 074509 (2012); doi: 10.1063/1.3702567

View online: <http://dx.doi.org/10.1063/1.3702567>

View Table of Contents: <http://jap.aip.org/resource/1/JAPIAU/v111/i7>

Published by the [American Institute of Physics](#).

---

### Related Articles

A readout for large arrays of microwave kinetic inductance detectors  
*Rev. Sci. Instrum.* **83**, 044702 (2012)

Positive-negative turbulence-free ghost imaging  
*Appl. Phys. Lett.* **100**, 131114 (2012)

Ultrahigh efficient single-crystalline TiO<sub>2</sub> nanorod photoconductors  
*Appl. Phys. Lett.* **100**, 123108 (2012)

Shift of responsive peak in GaN-based metal-insulator-semiconductor photodetectors  
*Appl. Phys. Lett.* **100**, 121109 (2012)

New Products  
*Rev. Sci. Instrum.* **83**, 039501 (2012)

---

### Additional information on J. Appl. Phys.

Journal Homepage: <http://jap.aip.org/>

Journal Information: [http://jap.aip.org/about/about\\_the\\_journal](http://jap.aip.org/about/about_the_journal)

Top downloads: [http://jap.aip.org/features/most\\_downloaded](http://jap.aip.org/features/most_downloaded)

Information for Authors: <http://jap.aip.org/authors>

## ADVERTISEMENT



**FIND THE NEEDLE IN THE  
HIRING HAYSTACK**

Post jobs and reach  
thousands of hard-to-find  
scientists with specific skills



<http://careers.physicstoday.org/post.cfm> **physicstoday** JOBS

## Atomic layer deposited Al<sub>2</sub>O<sub>3</sub> passivation of type II InAs/GaSb superlattice photodetectors

Omer Salihoglu,<sup>1,a)</sup> Abdullah Muti,<sup>1</sup> Kutlu Kutluer,<sup>2</sup> Tunay Tansel,<sup>2</sup> Rasit Turan,<sup>2</sup> Coskun Kocabas,<sup>1</sup> and Atilla Aydinli<sup>1</sup>

<sup>1</sup>Department of Physics, Bilkent University, 06800 Ankara, Turkey

<sup>2</sup>Department of Physics, Middle East Technical University, 06531 Ankara, Turkey

(Received 12 December 2011; accepted 8 March 2012; published online 9 April 2012)

Taking advantage of the favorable Gibbs free energies, atomic layer deposited (ALD) aluminum oxide (Al<sub>2</sub>O<sub>3</sub>) was used as a novel approach for passivation of type II InAs/GaSb superlattice (SL) midwave infrared (MWIR) single pixel photodetectors in a self cleaning process ( $\lambda_{\text{cut-off}} \sim 5.1 \mu\text{m}$ ). Al<sub>2</sub>O<sub>3</sub> passivated and unpassivated diodes were compared for their electrical and optical performances. For passivated diodes, the dark current density was improved by an order of magnitude at 77 K. The zero bias responsivity and detectivity was 1.33 A/W and  $1.9 \times 10^{13}$  Jones, respectively at 4  $\mu\text{m}$  and 77 K. Quantum efficiency (QE) was determined as %41 for these detectors. This conformal passivation technique is promising for focal plane array (FPA) applications. © 2012 American Institute of Physics. [<http://dx.doi.org/10.1063/1.3702567>]

### I. INTRODUCTION

A critical step in the fabrication of optoelectronic devices is the passivation of the exposed surfaces. Such surfaces are often created in order to confine current or light. In photodetectors, the requirement for the confinement of current is met by fabrication of a mesa structure, which results in a large number of surface states generated due to the abrupt termination of the crystal structure on the mesa side walls. Ensuing surface leakage currents are typically due to dangling bonds, inversion layers, and interfacial traps leading to lower responsivity. In photodetectors based on III-V materials, etched surfaces exposed to atmosphere form thin layers of native oxides some of which are good conductors, increasing the shunt current. Photodetectors with small pixel sizes (<25  $\mu\text{m}$ ) suffer from surface leakage more than large pixel photodetectors due to their higher perimeter to area ratio. Thus, for focal plane array (FPA) applications and long wavelengths, passivation becomes an especially vital issue. In order to overcome surface leakage currents, various passivation methods such as ammonium sulfide passivation,<sup>1,2</sup> deposition of silicon dioxide layer,<sup>3</sup> polyimide layer,<sup>4</sup> and overgrowth with wide bandgap material<sup>5</sup> have been used. Passivation is expected to suppress oxidation of the side walls and saturate dangling bonds to prevent surface states. Sulfur passivation replaces oxygen with sulfur at the mesa side walls and saturate the dangling bonds.<sup>2,6</sup> It is an effective passivation method and is relatively easy to apply but the effect of passivation is temporary and some reports claim that sulfur passivation damages the surface of the photodetector.<sup>6</sup> Silicon dioxide deposition on sidewalls have also been shown to be an effective technique, but it requires high temperatures for deposition or high RF powers to excite a plasma with potential for damage. With growth temperatures

of about 400 °C, high temperatures tend to damage III-V structures and high density energetic plasmas can cause physical damage on III-V surfaces and side walls resulting in unwanted surface states in the bandgap of the III-V materials. We note also that oxidation of the etched surfaces is typically very rapid and a thin layer of oxides forms almost immediately prior to passivation. Thus a self cleaning procedure eliminating the already formed thin oxide layer would be most welcome. Recent work on the surface and interface chemistry of III-V surfaces passivated with atomic layer deposited Al<sub>2</sub>O<sub>3</sub> has shown that it is possible to reduce the native oxides during deposition since formation of Al<sub>2</sub>O<sub>3</sub> is energetically preferred due to lower Gibbs free energy of Al<sub>2</sub>O<sub>3</sub> (−377.9 kcal/mol).<sup>7</sup> This is lower than the Gibbs free energies of Ga<sub>2</sub>O, Ga<sub>2</sub>O<sub>3</sub>, In<sub>2</sub>O<sub>3</sub>, As<sub>2</sub>O<sub>3</sub>, As<sub>2</sub>O<sub>5</sub>, and Sb<sub>2</sub>O<sub>3</sub>, which are −75.3 kcal/mol, −238.6 kcal/mol, −198.6 kcal/mol, −137.7 kcal/mol, −187.0 kcal/mol, and −151.5 kcal/mol, respectively.<sup>8,9</sup> Hinkle *et al.* using X-ray photoelectron spectroscopy (XPS) has shown that deposition of Al<sub>2</sub>O<sub>3</sub> on degreased and etched GaAs strongly reduces Ga and As oxides.<sup>10</sup> Similar work on InAs has shown strong reduction of In and As oxides.<sup>11</sup> Work on electrical characterization of MOS capacitors fabricated on GaSb has demonstrated strong suppression of Sb<sub>2</sub>O<sub>3</sub> due to Al<sub>2</sub>O<sub>3</sub> deposition.<sup>12</sup>

Surface passivation is even more critical in type-II superlattice (T2SL) InAs/GaSb photodetectors, due to a large number of very thin alternating layers. T2SL detectors have recently received great interest in the development of midwave and long wave infrared detectors due to advantages like bandgap engineering,<sup>13</sup> suppression of Auger recombination,<sup>14</sup> and interband tunneling<sup>15</sup> and has been shown to be a very promising alternative to MCT and QWIP in focal plane array (FPA) applications where, low dark current below 77 K is required.

In this work, we propose to use atomic layer deposited Al<sub>2</sub>O<sub>3</sub> as a passivation layer for InAs/GaSb SL photodetectors. ALD is a self limiting process that consists of sequential

<sup>a)</sup>Author to whom correspondence should be addressed. Electronic mail: omersalihoglu@yahoo.com, +903122901971.

gas phase reactions on the surface of the SL photodetector. The growth of  $\text{Al}_2\text{O}_3$  with ALD uses two gases that are introduced to the chamber one at a time and which react with the gas on the surface adsorbed during the previous sequence. ALD deposited  $\text{Al}_2\text{O}_3$  has many advantages as a passivation layer such as the control of thickness at the molecular level since in the ALD process, thickness depends on the number of reaction cycles. This leads to a precise thickness control as well as perfect conformal coverage even at sharp edges, large area thickness uniformity, very low process temperatures, and plasma free operation. Furthermore  $\text{Al}_2\text{O}_3$  is a very good dielectric over a very large frequency range. In the case of T2SL photodetectors where mesa etching leads to uneven etching of very thin InAs and GaSb layers at the side walls, conformal coverage at the atomic level may be very beneficial. These properties of ALD grown  $\text{Al}_2\text{O}_3$  make it a perfect candidate for passivation of InAs/GaSb super lattice FPA photodetectors. No use of  $\text{Al}_2\text{O}_3$  as a passivation layer has been made so far for InAs/GaSb super lattice system.

## II. EXPERIMENTAL

The sample studied in this work was grown commercially (IQE Inc. USA) with molecular beam epitaxy on a GaSb substrate. The photodetector is designed as p-i-n photodetector with design cutoff wavelength of  $5\ \mu\text{m}$ . It starts with 100 nm thick GaSb buffer layer and 20 nm  $\text{Al}_{(x)}\text{Ga}_{(y)}\text{Sb}$  as an insulator and etch stop layer, followed by 1000 nm GaSb:Be ( $p = 1.0 \times 10^{17}\ \text{cm}^{-3}$ ) p contact layer. P-i-n part of the design consist of 90 periods 8 monolayers (MLs) of InAs/8 MLs of GaSb:Be ( $p = 1.5 \times 10^{17}\ \text{cm}^{-3}$ ) p-type layers, 60 periods 8 MLs of InAs/8 MLs of GaSb i-layers, 60 periods 8 MLs of InAs:Te ( $n: 5 \times 10^{17}\ \text{cm}^{-3}$ )/8 MLs of GaSb n-type layers and structure is terminated by 20 nm InAs:Te ( $n: 5 \times 10^{17}\ \text{cm}^{-3}$ ) cap layer to assure good ohmic contact. Appropriate shutter sequences were applied to compensate the tensile strain caused by lattice mismatch between InAs and GaSb layers. Single pixel photodetectors were fabricated with  $400 \times 400\ \mu\text{m}$  mesa size. To minimize surface damage, mesas have been fabricated by standard lithography and wet etch solution. Mesa-isolated photodiodes are defined at room temperature, using the chemical solution based on  $\text{H}_3\text{PO}_4/\text{C}_6\text{H}_8\text{O}_7/\text{H}_2\text{O}_2/\text{H}_2\text{O}$  with 200 nm per minute etch rate. The etch process has been stopped when etch depth reached the bottom contact layer. The etch depth was about  $1.5\ \mu\text{m}$ . 200 cycles  $\text{Al}_2\text{O}_3$  passivation layer deposition carried out in atomic layer deposition system (Cambridge Nanotech Savannah 100) with  $150^\circ\text{C}$  as the substrate holder temperature. Growth of  $\text{Al}_2\text{O}_3$  has been done by delivering 0.015 s water vapor ( $\text{H}_2\text{O}$ ) and 0.015 s trimethylaluminum (TMA) pulses into the chamber in a sequential manner under constant 20 sccm  $\text{N}_2$  gas flow. A wait time of 20 s was added after each pulse to ensure surface reactions to take place. Both trimethylaluminum and water were unheated. The thickness of the film grown in this manner was determined as 20 nm by subsequent etching and measurement of the  $\text{Al}_2\text{O}_3$  film. Ohmic contacts were made by evaporating 5 nm Titanium (Ti) and 200 nm Gold (Au) on the bottom and top contact layers of the detectors. Fabricated detectors were bonded to a chip carrier

for further characterization. Exact same procedures were applied to another sample without  $\text{Al}_2\text{O}_3$  passivation to act as a reference detector.

## III. RESULTS AND DISCUSSION

To investigate the effect of  $\text{Al}_2\text{O}_3$  passivation, samples were mounted on a liquid nitrogen cooled cold finger. Dark current measurements were performed at 77 K by using a HP41420A source-measure unit. Figure 1 shows the measured dark current density versus applied bias voltage characteristics of the unpassivated and  $\text{Al}_2\text{O}_3$  passivated  $400 \times 400\ \mu\text{m}$  single pixel test diodes at 77 K. Single pixel passivated detector shows at least an order of magnitude reduction on dark current density compared with an unpassivated detector. At  $-0.1\ \text{V}$  bias voltage, dark current density reduced from  $4.7 \times 10^{-5}\ \text{A}/\text{cm}^2$  to  $6.6 \times 10^{-7}\ \text{A}/\text{cm}^2$ . These measurements yielded  $R_0A$  product values of  $1.6 \times 10^3\ \Omega\text{-cm}^2$  and  $3.7 \times 10^5\ \Omega\text{-cm}^2$  for the unpassivated and  $\text{Al}_2\text{O}_3$  passivated samples, respectively. At  $-0.1\ \text{V}$  bias and 77 K,  $\text{Al}_2\text{O}_3$  passivation shows improved dark current results when compared with  $\text{SiO}_2$  and SU8 passivation.<sup>6,16</sup> The prominent reduction in dark current due to ALD deposited  $\text{Al}_2\text{O}_3$  passivation is very encouraging for use in FPA applications.<sup>6,17</sup>

Spectral response of the photodetectors was measured using a Fourier transform infrared spectroscopy (Bruker Equinox 55) and a liquid nitrogen cooled cold finger system. Figure 2 shows spectral response of the unpassivated and  $\text{Al}_2\text{O}_3$  passivated photodetectors measured under single pass and front side illumination condition. The cut-off wavelength of the  $\text{Al}_2\text{O}_3$  passivated and unpassivated photodetectors is determined to be  $5.1\ \mu\text{m}$ .

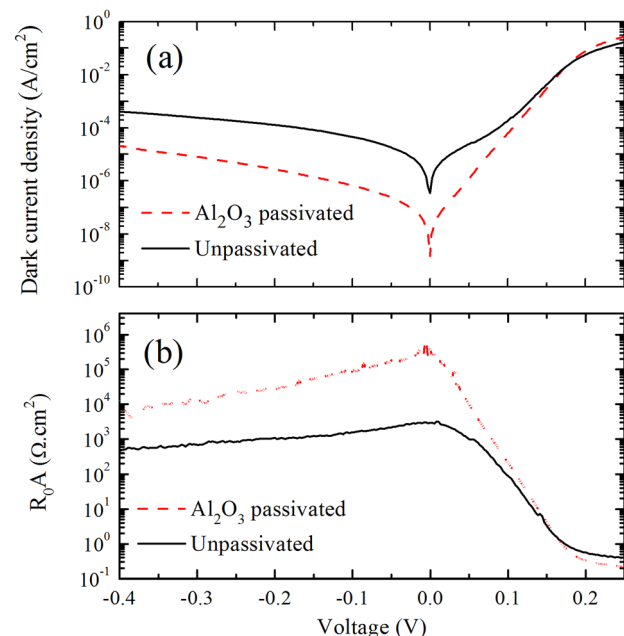


FIG. 1. (a) Dark current density vs applied bias of unpassivated and  $\text{Al}_2\text{O}_3$  passivated  $400\ \mu\text{m}$  single pixel square diodes measured at 77 K. (b) Zero bias differential resistance vs applied bias voltage characteristics for the unpassivated and  $\text{Al}_2\text{O}_3$  passivated samples at 77 K. Dashed line represents  $\text{Al}_2\text{O}_3$  passivated device and solid line represents unpassivated device.

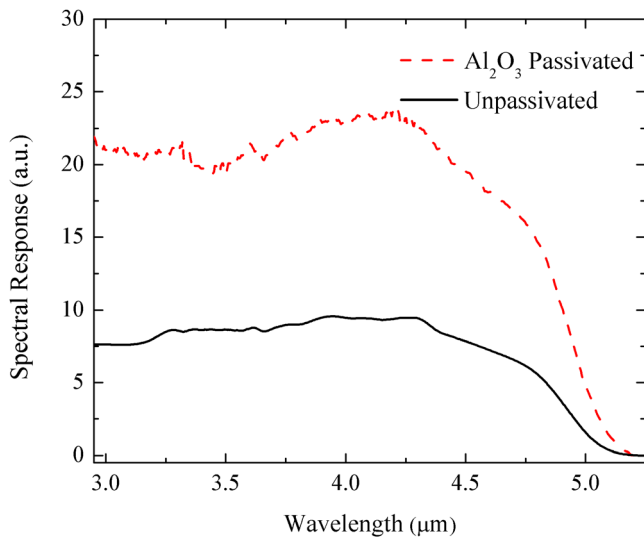


FIG. 2. Spectral response of the unpassivated and  $\text{Al}_2\text{O}_3$  passivated photodetectors at 77 K. The cut-off wavelength of the  $\text{Al}_2\text{O}_3$  passivated and unpassivated photodetectors is  $\sim 5.1 \mu\text{m}$ . Dashed line represents  $\text{Al}_2\text{O}_3$  passivated device and solid line represents unpassivated device.

The responsivity of the photodetectors has been measured at 77 K using calibrated blackbody source at  $800^\circ\text{C}$  (Newport, Oriel 67000), lock-in amplifier (SRS, SR830 DSP) and mechanical chopper (SRS, SR540) system. Photodetectors were illuminated with a 300 K background with a  $2\pi$  field-of-view. A 3-5  $\mu\text{m}$  blackbody filter has been used to eliminate unwanted illumination. Figure 3 shows responsivity and calculated Johnson-noise limited detectivity ( $D^*$ ) versus applied bias voltage graph for  $\text{Al}_2\text{O}_3$  passivated photodetector. The zero bias responsivity of  $\text{Al}_2\text{O}_3$  passivated photodetector was equal to 1.33 A/W at  $4 \mu\text{m}$  and 77 K. Under zero bias, the peak  $D^*$ , was equal to  $1.9 \times 10^{13}$  Jones for the  $\text{Al}_2\text{O}_3$  passivated single pixel photodetector at  $4 \mu\text{m}$  and 77 K. Quantum efficiency (QE) of the passivated photodetector has been determined as % 41 for single pass front illumination condition. When we compare our results with recent publications,<sup>6,16-19</sup> ALD grown  $\text{Al}_2\text{O}_3$  passivated

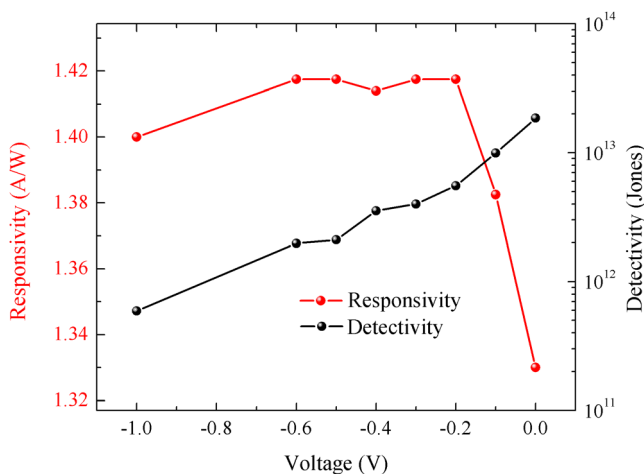


FIG. 3. Responsivity and detectivity of  $\text{Al}_2\text{O}_3$  passivated,  $400 \times 400 \mu\text{m}$  single pixel test detectors at 77 K and  $4 \mu\text{m}$ . The zero bias responsivity and the peak value of detectivity,  $D^*$  of  $\text{Al}_2\text{O}_3$  passivated photodetector was equal to 1.33 A/W and  $1.9 \times 10^{13}$  Jones, respectively.

T2SL photodetectors are very promising. In FPA applications, larger perimeter to area ratio increases the effect of surface leakage in the operation of the smaller FPA detectors and passivation becomes an important issue. ALD grown  $\text{Al}_2\text{O}_3$  passivation technique may be a good candidate also for LWIR photodetectors. This will be especially true for photodetectors designed to operate in the LWIR region due to relatively small bandgap of the LWIR photodetectors, where surface leakage currents are more dominant. Work is in progress to demonstrate this.

To understand the nature of the dark current, temperature dependent measurements of the dark current has been done. Relationship between the dark current densities and inverse temperatures at  $-0.1 \text{ V}$  bias are shown in Fig. 4. The I-V curve is dominated by diffusion current at high temperatures and generation-recombination current at low temperatures. The diodes with  $\text{Al}_2\text{O}_3$  passivation show lower dark current than unpassivated photodetectors at low temperatures. This indicates that the  $\text{Al}_2\text{O}_3$  passivation satisfies surface states and prevents current flow through the surface channel.  $\text{Al}_2\text{O}_3$  passivated photodetectors show Arrhenius type behavior above 100 K, characterizing the dominant bulk diffusion current. The activation energy has been calculated as 0.233 eV, which is close to the device bandgap. For lower temperatures the current begins to divert from the Arrhenius type of behavior. Generation recombination (G-R) current becomes dominant for mid temperatures. At 40 K dark current density shows a tendency to decrease indicating that surface leakage starts to become important in this temperature range.<sup>20</sup> For the unpassivated detector, dark current density deviates from the Arrhenius type of behavior at temperatures lower than 120 K indicating surface related currents are dominant at this range.

The influence of  $\text{Al}_2\text{O}_3$  on the performance of the T2SL is closely related to the interface chemistry of the  $\text{Al}_2\text{O}_3/\text{SL}$ . Components of InAs/GaSb SL are chemically very reactive. Their surfaces are easily oxidized and a native oxide layer of several nanometers thick is quickly formed upon exposure to air.<sup>21</sup> Oxygen diffuses through the surface, reacts with both

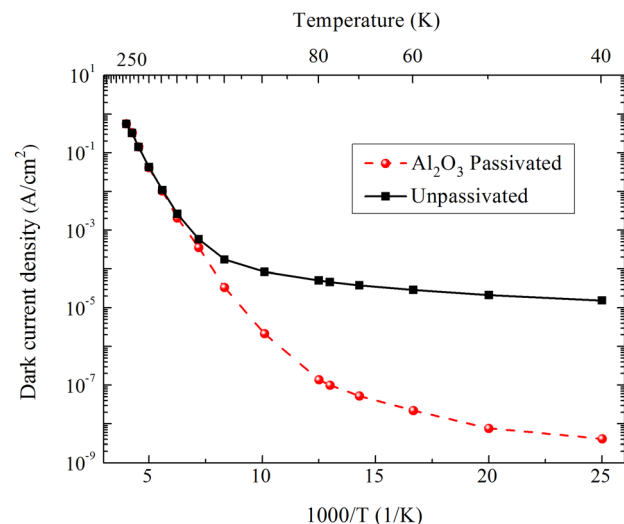


FIG. 4. Temperature dependent dark current measurements of  $\text{Al}_2\text{O}_3$  passivated and unpassivated photodetectors at  $-0.1 \text{ V}$  bias.

Ga and Sb, and forms oxide layers, through the chemical reaction  $2\text{GaSb} + 3\text{O}_2 \rightarrow \text{Ga}_2\text{O}_3 + \text{Sb}_2\text{O}_3$ .<sup>12</sup> Using the same argument leads to oxidation of In and As such that  $2\text{InAs} + 3\text{O}_2 \rightarrow \text{In}_2\text{O}_3 + \text{As}_2\text{O}_3$ .<sup>22</sup> Further,  $\text{In}_2\text{O}_3$  and  $\text{As}_2\text{O}_3$  may react and form  $\text{InAsO}_3$  (Ref. 23) since  $\text{In}_2\text{O}_3 + \text{As}_2\text{O}_3 \rightarrow 2\text{InAsO}_3$ . This mechanism is responsible for the formation of additional conductive channels and, consequently, leads to a large surface component of dark current. Reduction of the oxides during the ALD deposition is due to favorable Gibbs free energies for forming  $\text{Al}_2\text{O}_3$  compared to As, Ga, Sb, and In oxides.  $\text{Al}_2\text{O}_3$  formation is energetically preferred to native oxide of InAs and GaSb.

Alternatively,  $\text{Al}^{+3}$  atoms in the trimethylaluminum (TMA) molecule could possibly replace As atoms that form  $\text{As}_2\text{O}_3$  or In atoms in an  $\text{In}_2\text{O}_3$  molecule.<sup>24</sup> Similar reaction pathways with oxides of other metal atoms are also possible. These are so called interfacial self cleaning reactions of surface oxides.<sup>7</sup> Reduction of oxides after  $\text{Al}_2\text{O}_3$  deposition for GaSb and InAs has been confirmed by XPS measurements.<sup>11,12,25</sup>

Finally, in the case of T2SLs with large numbers of very thin dissimilar layers, different etch rates of InAs and GaSb lead to roughness on the mesa side walls. Conformal coating of atomic layer deposition creates a perfect protective layer against environmental effects especially against oxidation. This conformal coverage of rough surfaces also satisfies dangling bonds more efficiently while eliminating metal oxides in a self cleaning process. This makes ALD  $\text{Al}_2\text{O}_3$  a perfect candidate for passivation of InAs/GaSb superlattice photodetectors. That this state-of-art passivation technique results in high responsivity and detectivity and very low dark current is a clear indication of improvements due to self healing ALD  $\text{Al}_2\text{O}_3$  passivation process.

#### IV. CONCLUSION

In conclusion, we have demonstrated the suppression of dark current and increase in optical response of the InAs/GaSb superlattice photodetectors with cutoff wavelength at  $5.1 \mu\text{m}$  (MWIR). We have used ALD deposited  $\text{Al}_2\text{O}_3$  passivation layer on InAs/GaSb p-i-n design superlattice photodetectors. Plasma free and low operation temperature with uniform coating gave us conformal and defect free coverage on the side walls.  $\text{Al}_2\text{O}_3$  passivated superlattice photodetectors reduced the dark current from  $4.7 \times 10^{-5} \text{ A/cm}^2$  to  $6.6 \times 10^{-7} \text{ A/cm}^2$  compared to unpassivated photodetector at 77 K and under  $-0.1 \text{ V}$  applied bias condition. Corresponding zero bias area product ( $R_0A$ ) improved at least an order of magnitude (from  $1.6 \times 10^3 \Omega \cdot \text{cm}^2$  to  $3.7 \times 10^5 \Omega \cdot \text{cm}^2$ ). The zero bias responsivity and detectivity ( $D^*$ ) are determined as  $1.33 \text{ A/W}$  and  $1.9 \times 10^{13}$  Jones, respectively for the  $\text{Al}_2\text{O}_3$  passivated photodetector at  $4 \mu\text{m}$  and 77 K. Quantum efficiency (QE) of the passivated photodetector has been determined as % 41 for single pass front illumination condition.

Temperature dependent dark current measurements revealed that passivated devices show Arrhenius type of behavior at higher temperatures which is indication that dominant current is bulk diffusion current. The calculated activation energy is equal to 0.233 eV, which is close to the device bandgap. This work shows that ALD coated  $\text{Al}_2\text{O}_3$  is a good material as a passivation layer for p-i-n design InAs/GaSb superlattice photodetectors.

<sup>1</sup>E. Plis, J. B. Rodriguea, S. J. Lee, and S. Krishna, *Electron Lett.* **42**, 1248 (2006).

<sup>2</sup>V. N. Bessolov and M. V. Lebedev, *Semiconductors* **32**, 1141 (1998).

<sup>3</sup>A. Gin, Y. Wei, J. Bae, A. Hood, J. Nah, and M. Razeghi, *Thin Solid Films* **447**, 489 (2004).

<sup>4</sup>A. Hood, P. Y. Delaunay, D. Hoffman, M. Razeghi, and V. Nathan, *Appl. Phys. Lett.* **90**, 233513 (2007).

<sup>5</sup>R. Rehm, M. Walter, F. Fuchs, J. Schmitz, and J. Fleissner, *Appl. Phys. Lett.* **86**, 173501 (2005).

<sup>6</sup>H. S. Kim, E. Plis, A. Khoshaklagh, S. Mayers, N. Gautam, Y. D. Sharma, L. R. Dawson, S. Krishna, S. J. Lee, and S. K. Noh, *Appl. Phys. Lett.* **96**, 033502 (2010).

<sup>7</sup>D. Pulver, C. W. Wilmsen, D. Niles, and R. Kee, *J. Vac. Sci. Technol. B* **19**, 207 (2001).

<sup>8</sup>G. Hollinger, R. S. Kabbani, and M. Gendry, *Phys. Rev. B* **49**, 11159 (1994).

<sup>9</sup>A. J. Bard, R. Parsons, and J. Jordan, *Standard Potentials in Aqueous Solutions* (Marcel Dekker, New York, 1985).

<sup>10</sup>C. L. Hinkle, A. M. Sonnet, E. M. Vogel, S. McDonnel, G. J. Hughes, M. Milojevic, B. Lee, F. S. Aguirre-Tostado, K. J. Choi, H. C. Kim, J. Kim, and R. M. Wallace, *Appl. Phys. Lett.* **92**, 071901 (2008).

<sup>11</sup>R. Timm, A. Fian, M. Hjort, C. Thelander, E. Lind, J. N. Andersen, L. E. Wernersson, and A. Mikkelsen, *Appl. Phys. Lett.* **97**, 132904 (2010).

<sup>12</sup>A. Ali, H. S. Medan, A. P. Kirk, D. A. Zhao, D. A. Mourey, M. K. Hudait, R. M. Wallace, T. N. Jackson, B. R. Bennett, J. B. Boos, and S. Datta, *Appl. Phys. Lett.* **97**, 143502 (2010).

<sup>13</sup>Y. Wei and M. Razeghi, *Phys. Rev. B* **69**, 085316 (2004).

<sup>14</sup>C. H. Grein, P. M. Young, and H. Ehrenreich, *Appl. Phys. Lett.* **61**, 2905 (1992).

<sup>15</sup>D. L. Smith and C. Mailhot, *J. Appl. Phys.* **62**, 2545 (1987).

<sup>16</sup>M. Herrera, M. Chi, M. Bonds, N. D. Browning, J. N. Woolman, R. E. Kvaas, S. F. Harris, D. R. Rhiger, and C. J. Hill, *Appl. Phys. Lett.* **93**, 093106 (2008).

<sup>17</sup>H. S. Kim, E. Plis, J. B. Rodriguez, G. D. Bishop, Y. D. Sharma, L. R. Dawson, S. Krishna, J. Bundas, R. Cook, D. Burrows, R. Dennis, K. Patnaude, A. Reisinger, and M. Sundaram, *Appl. Phys. Lett.* **92**, 183502 (2008).

<sup>18</sup>E. Kwei-wei, D. Hoffman, B. M. Nguyen, P. Y. Delaunay, and M. Razeghi, *Appl. Phys. Lett.* **94**, 053506 (2009).

<sup>19</sup>R. Helm, M. Walter, J. Schmitz, F. Rutz, J. Fleibner, R. Scheibner, and J. Ziegler, *Infrared Phys. Technol.* **52**, 344 (2009).

<sup>20</sup>B. M. Nguyen, D. Hoffman, E. K. Huang, S. Bogdanov, P. Y. Delaunay, M. Razeghi, and Z. Tidrow, *Appl. Phys. Lett.* **94**, 223506 (2009).

<sup>21</sup>C. Cervera, J. B. Rodriguez, R. Chaghi, H. Ait-Kaci, and P. Christol, *J. Appl. Phys.* **106**, 024501 (2009).

<sup>22</sup>C. S. Seibert, M. D'Souza, J. C. Shin, L. J. Mawst, D. Botez, and D. C. Hall, *J. Appl. Phys.* **109**, 033103 (2011).

<sup>23</sup>G. Hollinger, R. Skheyta-Kabbani, and M. Gendry, *Phys. Rev. B* **49**, 11159 (2004).

<sup>24</sup>C. H. Chang, Y. K. Chiou, Y. C. Chang, K. Y. Lee, T. D. Lin, T. B. Wu, M. Hong, and J. Kwo, *Appl. Phys. Lett.* **89**, 242911 (2006).

<sup>25</sup>H. D. Trinh, G. Brammertz, E. Y. Chang, C. I. Kuo, C. Y. Lu, Y. C. Lin, H. Q. Nguyen, Y. Y. Wong, B. T. Tran, K. Kakushima, and H. Iwai, *IEEE Elec. Dev. Lett.* **32**, 752 (2011).